ARMAR-4: A 63 DOF Torque Controlled Humanoid Robot

Tamim Asfour, Julian Schill, Heiner Peters, Cornelius Klas, Jens Bücker,
Christian Sander, Stefan Schulz, Artem Kargov, Tino Werner, Volker Bartenbach

***Abstract*— We present the mechatronic design of the next generation of our humanoid robots, the humanoid robot ARMAR-4, a full body torque controlled humanoid robot with 63 active degrees of freedom, 63 actuators, 214 sensors, 76 microcontroller for low-level control, 3 PCs for perception, high-level control and balancing, a weight of 70 kg including batteries and total height of 170 cm. In designing the robot we follow an integrated approach towards the implementation of high performance humanoid robot systems, able to act and interact in the real world using only on-board sensors and computation power. Special attention was paid to the realization of advanced bimanual manipulation and locomotion capabilities. The paper presents the design concept of the robot and its mechatronic realization.**

I. INTRODUCTION AND RELATED WORK

Humanoid robotics is an emerging and challenging research field, which has received significant attention during the past years and will continue to play a central role in robotics research and many applications of the 21st century. Regardless of the application area, one of the common problems tackled in humanoid robotics is the understanding of human-like information processing and the underlying mechanisms of the human brain in dealing with the real world.

Considerable progress has been made in humanoid research resulting in a number of humanoid robots able to move and perform well-designed tasks. Over the past decade in humanoid research, an encouraging spectrum of science and technology has emerged that leads to the development of highly advanced humanoid mechatronic systems endowed with rich and complex sensorimotor capabilities. This include ASIMO [1], HRP-2 [2], HRP-4C [3], HRP4 [4], Toyota's partner robot [5], DB [6], CB [7], ARMAR [8], iCub [9], COMAN[10], NAO [11], DARwIn-OP [12], WABIAN-2 [13], KOBIAN [14], Twendy-One [15], HUBO [16], Justin [17] and DLR humanoid [18], Lola [19], REEM [20], Robonaut [21], and Petman [22] to name a few. Of major importance for advances of the field is without doubt the availability of reproducible humanoid robot systems (HRP-2, NAO, HUBO, iCub), which have been used in the last years as common hardware and software platforms to support humanoids research. Many technical innovations and remarkable results by universities, research institutions and companies are visible.

Ambitious goals have been set for future humanoid robotics. They are expected to serve as companions and assistants for humans in daily life and as ultimate helpers in man-made and natural disasters. In 2050, a team of humanoid robots soccer players shall win against the winner of most recent World Cup. DARPA announced recently the next Grand Challenge in robotics: building robots which do things like humans in a world made for humans. The research roadmap for humanoid robotics in the next years could be structured around two major groups of disciplines: driving disciplines which provide the ideas and motivation for research, and technological disciplines, which provide the necessary enabling technologies.

Fig. 1. The humanoid robot ARMAR-4: torque controlled humanoid robot with 63 active degrees of freedom, 63 actuators, 214 sensors, 76 microcontroller, 3 PCs, 70 kg and 170 cm.

From our perspective, the important research directions toward complete humanoids robot systems, which are able to act and interact in the real world to perform a wide variety of tasks are

- Humanoid mechatronics with human like performance

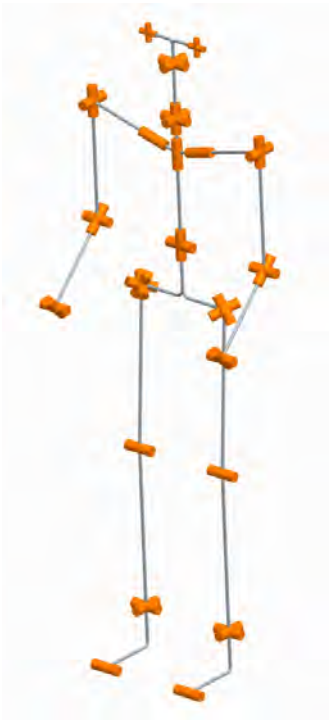

Fig. 2. The kinematic structure or ARMAR-4: head with 9 DOF, each arm with 8 DOF, each leg 7 DOF, hip with 2 DOF and each hand with 11 DOF (not shown in the figure)

regarding dexterity, force capabilities, energy efficiency and compliance.

- Humanoid control strategies able to deal with high-dimensionality, redundancy and unexpected disturbances.
- Humanoid cognitive architectures which integrate perception, action, reasoning, learning, interactions and communication.

Research in these directions will push forward the closeness of humanoid robots to humans in terms of embodiment, performance, interaction, communication, cooperation and assistance capabilities as well as social embedding. In this paper we present a new humanoid robot ARMAR-4 with advanced mechatronics towards higher performance regarding dexterous manipulation and locomotion capabilities.

II. DESIGN AND MECHATRONICS OF ARMAR-4

From the kinematic control point of view, the robot consists of eight subsystems: head, left arm, right arm, left hand, right hand, torso, left leg and right leg. The kinematic structure of the robot is shown in Fig. 2. The robot has been designed to be modular and light-weight while retaining similar size and proportion as an average person of 170 cm and 70 kg. The DH parameters of the robot are given in the table I, II and III. In the following we give a short description of the main innovations in the design of the robot.

A. Head

The head has been developed based on our experience on building the humanoid robot ARMAR-III [8] and the Karlsruhe active humanoid head [23]. The head has nine DOF and is equipped with two eyes. The eyes execute independent pan and tilt movements. Each eye is equipped with two digital color cameras (wide and narrow angle). The visual system is mounted on a five DOF neck mechanism for lower and upper pitch, lower and upper roll and yaw.

TABLE I

DH PARAMETERS OF THE LEGS

Joint:	$\theta[^\circ]$	$\alpha[^\circ]$	a [mm]	d [mm]
0	θ_0	α_0	a_0	d_0
1	$-90+\theta_1$	90	0	0
2	$90+\theta_2$	90	0	2.3
3	$51.897+\theta_3$	125.235	229.334	353.753
4	$-39.545+\theta_4$	90	401.724	93.514
5	θ_5	90	0	74.092
6	$119.625+\theta_6$	0	150.707	119.625

TABLE II

DH PARAMETERS OF THE ARMS

Joint:	$\theta[^\circ]$	$\alpha[^\circ]$	a [mm]	d [mm]
0	0	0	a_0	d_0
1	$90+\theta_1$	90	0	0
2	$90+\theta_2$	0	a_2	d_2
3	θ_3	75	0	0
4	$-90+\theta_4$	90	53.69	200
5	$105+\theta_5$	90	0	0
6	$-90+\theta_6$	-90	0	300
7	θ_7	90	0	0
8	$90+\theta_8$	90	0	250
9	$-90+\theta_9$	90	0	0

TABLE III

DH PARAMETERS OF THE HEAD

Joint:	$\theta[^\circ]$	$\alpha[^\circ]$	a [mm]	d [mm]
0	0	0	a_0	d_0
1	$90+\theta_1$	90	0	0
2	$-90+\theta_2$	-90	a_2	d_2
3	θ_3	90	0	0
4	$-90+\theta_4$	90	0	0
5	$90+\theta_5$	90	0	140
6	$90+\theta_6$	-90	0	0
7	θ_7	90	72.65	58.5
8	$-90+\theta_8$	-90	0	46.5
9	θ_9	-90	72.65	58.5
10	$90+\theta_{10}$	90	0	46.5

B. Arm

The arm has been developed to increase dexterity in bimanual manipulation tasks. Based on the human arm model developed in [24] and the manipulability analysis [25] of the human arm kinematics, we realized one of the inner shoulder joints (articulatio sternoclavicularis) in addition to the standard 7 DOF in humanoid arms. The axis of the inner shoulder joints for the left and right arm coincide in the center between the outer shoulder joints. This joint is realized using a sliding joint actuated by the same driving unit. This results in a 8 DOF humanoid arm (see Fig. 4) with an increased dexterity in areas in front of the robot leading to significantly higher number of configurations and thus higher dexterity when performing bimanual manipulation tasks. From kinematic point of view, through the additional

Fig. 3. 9 DOF head of ARMAR-IV: independent eye pan and tilt, lower and upper pitch, lower and roll and yaw. For cameras and six microphones.

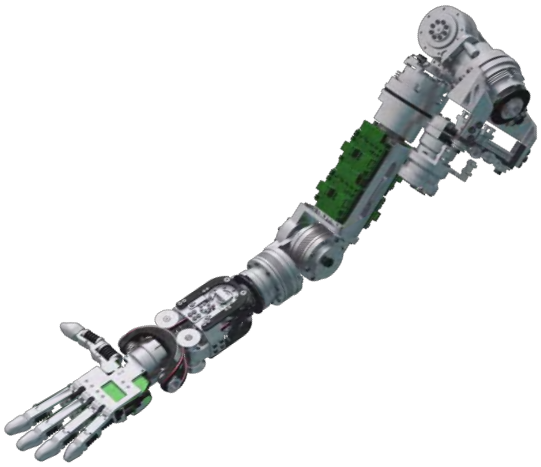

Fig. 4. 8 DOF arm of ARMAR-IV: In addition to classical 7 DOF humanoid robot arms, an additional DOF of the inner shoulder joint was realized according to the human arm model developed in [24] and based on manipulability analysis [25] to improve dexterity in particular in the case of bimanual manipulation.

inner shoulder joint the maximum of the manipulability index of an human-like arm is moved towards the center of the body.

All joints are realized by driving units developed to be modular and usable for the different joints of the robot. The driving units combine motor, harmonic drive, incremental and absolute joint position measurements, torque and temperature. Details of the driving units will be described in section II-D.2. Each arm has a 6 DOF force/torque sensor in the wrist. The wrist joint has been designed to allow the allocation of the force/torque sensor in the intersection of the wrist joints. For details of the wrists mechanism, the reader is referred to [26].

C. Hands

The design of the hand is based on our experience with compliant fluidic actuated hands we made in the design of the hands for ARMAR-III [27]. The advantages of fluidic actuators are a high power to weight ratio and a safe interaction with humans and objects due to the inherent compliance. New flexible fluidic actuators [28] have been used, which withstand much more load cycles. The hand has the size of a human hand and a weight of 450g. Each finger of the hand has two DOF and the thumb can be moved in opposition, which results in 11 DOF per hand. As the 2 DOF of the ring and pinky finger are coupled only 9 DOF can be controlled individually, though. The joints are pneumatically actuated with 4 bar over pressure and 1 bar under pressure. There are absolute position encoders and air pressure sensors in each joint, which allows us to realize a force position control by measuring the angle and air pressure and controlling it with a model based approach [29]. The complete control electronics, sensors and valves have been integrated in the hand, so that only air pressure, CAN-Bus and power has to be connected. This leads to fewer wiring in the wrist and more space in the under arm.

Fig. 5. 11 DOF humanoid hand actuated by fluidic actuators. The actuators are connected to on-board over pressure and under pressure tanks to allow fast and controlled closing and opening of the fingers

D. Legs

In designing the legs, the basic requirements were to have a highly integrated design with advanced capabilities in terms of joint torques and human-like walking styles.

1) Leg Design: The legs of the humanoid robot ARMAR-4 are designed with 7 DOF each. There are 3 DOF in the hip, 1 in the knee, 2 in the ankle and 1 DOF at the toes. The structural parts are made of an aluminium alloy and optimized using FEM-based CAE-optimization. Installation space of the entire design is aligned to a body-model of

a 170 cm human body. The weight of each leg is 12 kg in complete. Except for the toe joints, every joint is actuated by the same uniform drive unit, which integrates measurement for torque, angle and temperature. The parameters of the legs are given in table IV.

2) Driving Unit: The universal drive unit is specially designed for being used in all the joints of the legs except for the toes, dramatically reducing the number of different parts and simplifying control. The overall weight of one unit is 1.3 kg. It offers a high maximum torque of 157 Nm, while it is able to move at a maximum angular speed of 336 degree/s. The motors used inside are RoboDrive RD85 [30] BLDC motors, because of their high power-to-weight ratio. For the gears Harmonic Drive CPL25 were chosen with a transmission of 100:1. On the stator, a temperature sensor is mounted for saving the motor from over-heating, whereas cooling is achieved passively by cooling fins on the outside of the drive unit. For torque measurement a spoke wheel is used. Angular measurement is done incrementally for commutation and again absolutely on the output axis. Bearing is done by one single cross-roller bearing.

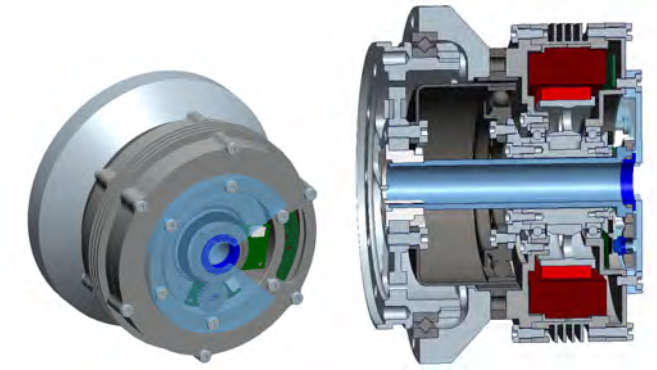

Fig. 6. Driving unit integrating motor, gear, incremental and absolute position sensors, torque and temperature sensors. To reduce costs, the design or the unit was optimized to reduce the number of mechanical parts resulting in only 11 mechanical parts needed to produce the driving unit.

3) Hip joint: As mentioned before, the hip is actuated by three drive units (see Fig. 8). All three rotation axes are crossing in one intersection point. However, one of the drive units is displaced in parallel to succeed installation space conditions. Forces are transmitted to the joint axis by steel bar-connected joint heads, allowing pushing as well as pulling for inhibiting high radial loads on the joint bearing. The joint axes are first arranged in a 45 degree angular displacement according to the roll axis. This displacement is resulting in a torque gain of $\sqrt{2}\cdot\tau = 222$ Nm for movements in direction of pitch and roll, where $\tau = 157$ Nm is the maximum torque of the driving unit. Another rotation of the new axis by 45 degree is increasing torque gain for pitch or roll movement out of the initial position to $\sqrt{3}\cdot\tau = 272$ Nm, as for these directions now all three drive units operate at a time. The further the joints get moved in pitch or roll axis, the lower the torque gain of that DOF will be, resulting in a minimum of 1. The sum of all hip joint torques possible at a time always stays constant.

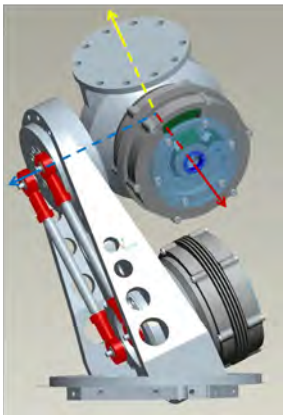

Fig. 7. The hip joints: All three joints intersect in a single point and are coupled to achieve the required high torques.

4) Knee joint: The knee joint is driven by one single drive unit which is supported by two springs mounted inside the upper leg. The springs are arranged serially by a bowden-cable connection and a deflection pulley. According to the drive unit the spring-setup is attached in parallel. When the knee gets bent, the springs are preloaded and can release the power when stretching the knee again. Thus, power-consumption while walking can be reduced and maximum torque is increased to 247 Nm. Furthermore, power-consumption while standing will be less, as the springs' preload is designed to compensate the body-weight.

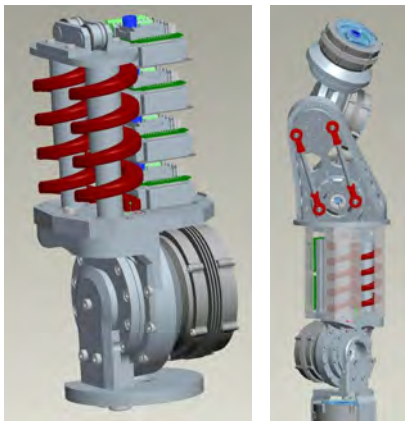

Fig. 8. The knee joint: The same driving unit is used with parallel springs.

5) Ankle joints: At the ankle joints the two drive units are aligned facing each other in the calf to obtain installation space requirements (see Fig.10). Torque is transmitted towards concentric axes in between the drive units by bowden-cables. On these axes, joint heads are mounted, transmitting the power to joint heads on the ankle using steel bars. This differential actuation doubles the torque for ankle movements. However, it is not exactly twice the torque for pitch movement because of different lengths of lever arms at the joint head pairs. Again, the joint axes share one intersecting point. Between the joint axes and the foot a 6D force/torque sensor is mounted.

TABLE IV
LEG PARAMETERS

Joint		Cont. torque [Nm]	Max. torque [Nm]	Max. angular speed [degree/s]	Range of motion [degree]
Hip	roll	75-130	157–271	336	[-45, 55]
	pitch	75-130	157–271	336	[-25, 70]
	yaw	75-130	157–271	336	[-50, 60]
Knee	pitch	75-165	157–247	336	[-110, 0]
Ankle	roll	150	314	336	[-12, 12]
	pitch	126	264	400	[-50, 60]
Toe	pitch		6	–	–

6) Feet: The feet are equipped with seven force sensors on the sole each. For toe movement one gear-motor is attached to the two toes by a belt, whereas the two toes' joint axes are connected by a cardan joint. There is a passive spring-loaded joint in the heel, which is elastic to reduce the impact while walking.

III. CONTROL ARCHITECTURE

A. Motor Control System

The joints in the legs, arms and torso are actuated by brushless DC electric motors, which are controlled by off-the-shelf digital servo drives from Elmo Motion Control [31]. The servo drives have been complemented with a custom PCB, which carries the connectors for power, motors, sensors and communication as well as a dsPIC33 microcontroller from Microchip, which is used for absolute angle measurement, torque measurement and temperature monitoring. The microcontroller is able to communicate with the servo drive via RS232 and CAN-Bus. The DC motors in the head and toes are controlled by a custom motor control board, which can control up to four motors with a maximum current of 5 amperes per motor.

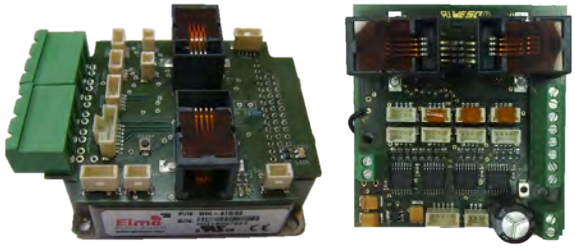

Fig. 9. Elmo Whistle Servo Drive with custom PCB (left) for control of one BLDC motor and the DC motor controller (right), which can control up to 4 DC motors.

B. Sensors

Each joint is equipped with an an incremental motor encoder and an absolute joint encoder. These are realized by rotary magnetic position sensors from ams [32], which use a hall sensor array to measure the orientation of a rotating magnet and have a resolution of 12 bit. The absolute joint encoders make a reset movement, where the robot moves to the zero position of each joint, unnecessary. Torque and motor temperature measurement is implemented in each joint of the arms and legs. Torque is measured by strain gauges which have been applied on a shaft or a spoke wheel in the drive unit. The temperature is measured by PT1000 elements which have been integrated in the stators of the motors. In each foot there are seven strain gauge load cells, which measure the force distribution of the foot to the ground (see Fig. 10). 6 DOF force/torque sensors are mounted in each wrist and each ankle. In the head one foveal and one perspective stereo camera pair with a resolution of 640x480 are mounted. Two inertial measurement units have been integrated in the head and the hip. Table V shows an overview over the sensors integrated in the robot.

TABLE VI
OVERVIEW OVER THE MOTORS

Type	Manufacturer	Position	Quantity
RD25	robodrive [30]	Wrists	4
RD38	robodrive [30]	Shoulders	2
RD50	robodrive [30]	Upper Arms	10
RD70x18	robodrive [30]	Torso	2
RD85	robodrive [30]	Legs	12
2342 CR	Faulhaber [33]	Head	2
2224 SR	Faulhaber [33]	Head	3
2225 SR	Faulhaber [33]	Head	1
2226 SR	Faulhaber [33]	Head	1
1524	Faulhaber [33]	Eyes	2
2642 W	Faulhaber [33]	Toes	2

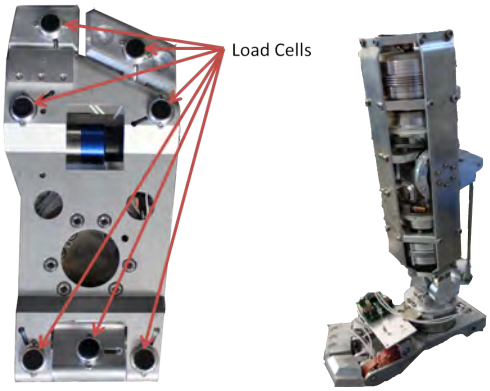

Fig. 10. Distribution of the load cells in the foot (left) and assembly of the lower leg and the ankle joint (right)

C. PC system

There are three PC/104 computers in the robot: Two are positioned in the torso and one in the head. The PC/104 in the head is equipped with an Intel Core2Duo processor

TABLE V
OVERVIEW OVER THE SENSORS

Sensor	Type	Manufacturer	Properties	Position	Quantity
Incremental encoders	AS5306	ams [32]	11520 steps/rev.	Legs and upper arms	22
	AS5145	ams [32]	4096 steps/rev.	Lower arms, torso pitch	7
	MR-Sensor	Robodrive [30]	30720 steps/rev.	Torso yaw	1
	IE2-512	Faulhaber [33]	512 steps/rev.	DC motors in head and toes	11
Absolute encoders	AS5145	ams [32]	4096 steps/rev.	Every joint, except toes	61
Temperature sensors	PT1000			Motors in legs, arms and torso	30
Spoke wheel	Custom	ME-Mesysteme GmbH [34]	200Nm, 2mV/V	Leg drive units, torso joints	14
Torque sensor shafts	Custom			Arm drives	16
Load cells				Shoulder	4
Load cells	ELAF	measurement specialities [35]	1250N, 20mV/V	Feet	14
6 DOF Force/torque wrist	Mini45	ATI-IA [36]	145N, 5Nm	Wrist	2
6 DOF Force/torque ankle	Omega85	ATI-IA [36]	2000N, 100Nm	Ankle	2
Cameras	Dragonfly 2	Point Grey Research [37]	Firewire, 0.3MP, 60fps	Head	4
IMUs	ThinIMU	Scinamics [38]		Head and Hip	2
Hand air pressure sensors	MS5803	measurement specialities [35]	6 bar, 24 bit	Hands	20
Microphones	ME15	Olympus [39]		Head	6

and a combined audio and Firewire board. It is used for computer vision and sound processing. In the torso there are two PC/104s. One is equipped with an Intel Core i7 processor and is performing the high level planning and control, the other one is equipped with an Intel Core2Duo processor and a PCI/104 10 channel CAN interface board, running a Xenomai real time operating system and is used for low level control and communication with the sensors and motor controllers.

D. Communication

Fig. 11 shows the communication architecture of the control system. The PCs are communicating via Gigabit Ethernet and a link to the outside world can be established via Ethernet or IEEE 802.11n WLAN. As all PCs are equipped two Ethernet interfaces, which can be run bridged mode, no Ethernet switch is needed. All sensors and controllers are connected to the low level control PC via six CAN busses: One for each leg and arm, one for the head and one for the torso. For the communication over CAN we use the CANopen protocol with a baudrate of 1 Mbps, which allows real time control with low overhead. The four cameras are connected with two Firewire busses, which are split up with two Firewire hubs. The IMUs are connected via USB to the head PC and the low level control PC.

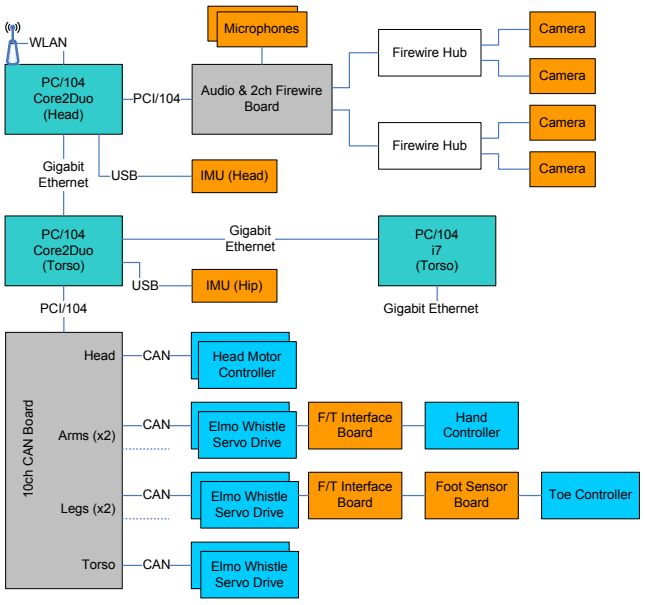

Fig. 11. Computer architecture of ARMAR-4

IV. RESULTS AND FUTURE WORK

We presented the current status of the realization of the mechatronics of the humanoid robot ARMAR-4. The assembly, cabling and wiring is finished. The robot is shown in Fig. 12. First tests of the low level control have been completed. Our kinematics analysis shows that the new leg design will allow the implementation of human-like walking styles such as CatWalk. Future work will concentrate on transferring the grasping and manipulation capabilities of ARMAR-III to the new robot and the investigation of push recovery and safe falling strategies.

ACKNOWLEDGMENT

This work was supported by the German Research Foundation (Deutsche Forschungsgemeinschaft: DFG) through the Collaborative Research Project on Humanoid Robots (SFB 588). The authors would like to thank many people who contributed in the different phases to the development of ARMAR-4. In particular, the authors thank Rüdiger Dillmann, Paul Holz, Jonas Beil, Wolfgang Burger, Georg Bretthauer, Albert Albers, and all members of the humanoids group at KIT and of the SFB588.

REFERENCES

[1] Y. Sakagami, R. Watanabe, C. Aoyama, S. Matsunaga, N. Higaki, and K. Fujimura, "The intelligent ASIMO: system overview and integration," in *IEEE/RSJ International Conference on Intelligent Robots and Systems (IROS)*, vol. 3, 2002, pp. 2478–2483 vol.3.

[2] K. Kaneko, F. Kanehiro, S. Kajita, H. Hirukawa, T. Kawasaki, M. Hirata, K. Akachi, and T. Isozumi, "Humanoid robot HRP-2," in *IEEE International Conference on Robotics and Automation (ICRA)*, vol. 2, 2004, pp. 1083–1090 Vol.2.

[3] K. Kaneko, F. Kanehiro, M. Morisawa, K. Miura, S. Nakaoka, and S. Kajita, "Cybernetic human HRP-4C," in *IEEE/RAS International Conference on Humanoid Robots (Humanoids)*, 2009, pp. 7–14.

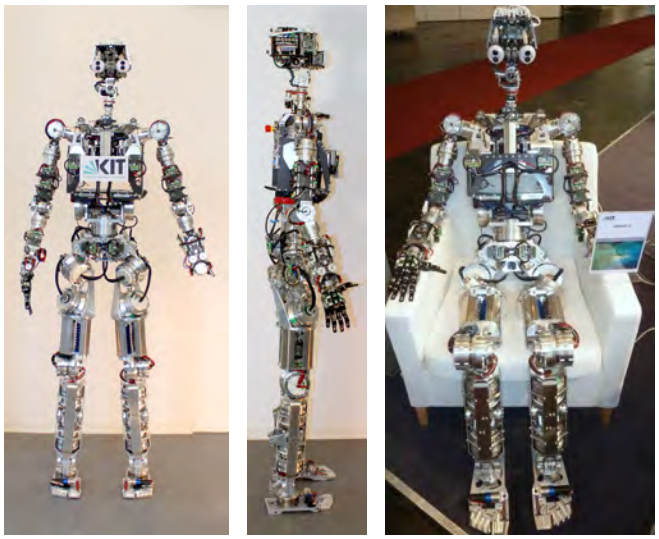

Fig. 12. The humanoid robot ARMAR-4

[4] K. Kaneko, F. Kanehiro, M. Morisawa, K. Akachi, G. Miyamori, A. Hayashi, and N. Kanehira, "Humanoid robot HRP-4 - Humanoid robotics platform with lightweight and slim body," in *IEEE/RSJ International Conference on Intelligent Robots and Systems (IROS)*, 2011, pp. 4400–4407.

[5] "Toyota," http://en.wikipedia.org/wiki/Toyota_Partner_Robot.

[6] C. Atkeson, J. Hale, F. Pollick, M. Riley, S. Kotosaka, S. Schaul, T. Shibata, G. Tevatia, A. Ude, S. Vijayakumar, E. Kawato, and M. Kawato, "Using humanoid robots to study human behavior," *Intelligent Systems and their Applications, IEEE*, vol. 15, no. 4, pp. 46–56, 2000.

[7] G. Cheng, S. Hyon, J. Morimoto, A. Ude, G. Colvin, W. Scroggin, and S. Jacobsen, "CB: A Humanoid Research Platform for Exploring NeuroScience," in *IEEE/RAS International Conference on Humanoid Robots (Humanoids)*, 2006, pp. 182–187.

[8] T. Asfour, K. Regenstein, P. Azad, J. Schröder, N. Vahrenkamp, and R. Dillmann, "ARMAR-III: An Integrated Humanoid Platform for Sensory-Motor Control," in *IEEE/RAS International Conference on Humanoid Robots (Humanoids)*, Genova, Italy, December 2006, pp. 169–175.

[9] G. Metta, G. Sandini, D. Vernon, L. Natale, and F. Nori, "The iCub humanoid robot: an open platform for research in embodied cognition," in *Proceedings of the 8th workshop on performance metrics for intelligent systems*. ACM, 2008, pp. 50–56.

[10] N. G. Tsagarakis, S. Morfey, G. A. Medrano-Cerda, Z. Li, and D. Caldwell, "COMAN a Compliant Humanoid: Optimal Joint Stiffness Tuning for Modal Frequency Control," in *IEEE International Conference on Robotics and Automation (ICRA)*, 2013.

[11] "Aldebaran," http://www.aldebaran-robotics.com/en/.

[12] "Robotis," http://www.robotis.com/xe/darwin_en.

[13] Y. Ogura, H. Aikawa, K. Shimomura, A. Morishima, H. ok Lim, and A. Takanishi, "Development of a new humanoid robot WABIAN-2," in *IEEE International Conference on Robotics and Automation (ICRA)*, 2006, pp. 76–81.

[14] M. Zecca, N. Endo, S. Momoki, K. Itoh, and A. Takanishi, "Design of the humanoid robot KOBIAN - preliminary analysis of facial and whole body emotion expression capabilities-," in *IEEE/RAS International Conference on Humanoid Robots (Humanoids)*, 2008, pp. 487–492.

[15] H. Iwata and S. Sugano, "Design of human symbiotic robot TWENDY-ONE," in *IEEE International Conference on Robotics and Automation (ICRA)*, 2009, pp. 580–586.

[16] J. Lee, J.-Y. Kim, I.-W. Park, B.-K. Cho, M.-S. Kim, I. Kim, and J.-H. Oh, "Development of a Humanoid Robot Platform HUBO FX-1," in *SICE-ICASE, 2006. International Joint Conference*, 2006, pp. 1190–1194.

[17] T. Wimböck, C. Borst, A. Albu-Schäffer, C. Ott, C. Schmidt, M. Fuchs, W. Friedl, O. Eiberger, A. Baumann, A. Beyer, and G. Hirzinger, "DLR's Two-Handed Humanoid Justin: System Design, Integration, and Control," *at-Automatisierungstechnik*, vol. 58, no. 11, pp. 622–628, 2010.

[18] C. Ott, O. Eiberger, J. Englsberger, M. A. Roa, and A. Albu-Schäffer, "Hardware and Control Concept for an Experimental Bipedal Robot with Joint Torque Sensors," *Journal of the Robotics Society of Japan*, vol. 30, no. 4, pp. 378–382, 2012.

[19] S. Lohmeier, T. Buschmann, and H. Ulbrich, "Humanoid robot LOLA," in *IEEE International Conference on Robotics and Automation (ICRA)*, 2009, pp. 775–780.

[20] R. Tellez, F. Ferro, S. Garcia, E. Gomez, E. Jorge, D. Mora, D. Pinyol, J. Oliver, O. Torres, J. Velazquez, and D. Faconti, "Reem-B: An autonomous lightweight human-size humanoid robot," in *IEEE/RAS International Conference on Humanoid Robots (Humanoids)*, 2008, pp. 462–468.

[21] R. O. Ambrose, H. Aldridge, R. S. Askew, R. R. Burridge, W. Bluethmann, M. Diftler, C. Lovchik, D. Magruder, and F. Rehnmark, "Robonaut: NASA's space humanoid," *Intelligent Systems and their Applications, IEEE*, vol. 15, no. 4, pp. 57–63, 2000.

[22] "Boston Dynamics," http://www.bostondynamics.com/.

[23] T. Asfour, K. Welke, P. Azad, A. Ude, and R. Dillmann, "The Karlsruhe Humanoid Head," in *IEEE/RAS International Conference on Humanoid Robots (Humanoids)*, Daejeon, Korea, December 2008, pp. 447–453.

[24] T. Asfour, "Sensormotorische Koordination für die Handlungsausführung eines humanoiden Roboters (in German)," Ph.D. dissertation, Universität Karlsruhe (TH), Karlsruhe, Germany, May 2003.

[25] T. Yoshikawa, "Manipulability of Robotic Mechanisms," *The International Journal of Robotics Research*, vol. 4, no. 2, pp. 3–9, 1985.

[26] A. Albers, J. Ottnad, and C. Sander, "Development of a new wrist for the next generation of the humanoid robot ARMAR," in *IEEE/RAS International Conference on Humanoid Robots (Humanoids)*, 2008, pp. 46–53.

[27] I. Gaiser, S. Schulz, A. Kargov, H. Klosek, A. Bierbaum, C. Pylatiuk, R. Oberle, T. Werner, T. Asfour, G. Bretthauer, and R. Dillmann, "A new anthropomorphic robotic hand," in *IEEE/RAS International Conference on Humanoid Robots (Humanoids)*, 2008, pp. 418–422.

[28] I. Gaiser, S. Schulz, H. Breitwieser, and G. Bretthauer, "Enhanced Flexible Fluidic actuators for biologically inspired lightweight robots with inherent compliance," in *IEEE International Conference on Robotics and Biomimetics (ROBIO)*, 2010, pp. 1423–1428.

[29] A. Bierbaum, J. Schill, T. Asfour, and R. Dillmann, "Force Position Control for a Pneumatic Anthropomorphic Hand," in *IEEE/RAS International Conference on Humanoid Robots (Humanoids)*, Paris, France, 2009, pp. 21–27.

[30] "Robodrive," http://www.robodrive.de/.

[31] "Elmo Motion Control - Servo Drives," http://www.elmomc.com/ http://www.elmomc.com/products/elmo-digital-servo-drives-main.htm.

[32] "ams AG," http://www.ams.com/ http://www.ams.com/eng/Products/Magnetic-Position-Sensors/Linear-Incremental-Magnetic-Position-Sensors/AS5306 http://www.ams.com/eng/Products/Magnetic-Position-Sensors/Rotary-Magnetic-Position-Sensors/AS5145H.

[33] "Faulhaber," http://www.faulhaber.com/.

[34] "ME-Systeme," http://www.me-systeme.de.

[35] "measurement specialities," http://www.meas-spec.com http://www.meas-spec.com/product/t_product.aspx?id=2418 http://www.meas-spec.com/product/pressure/MS5803-05BA.aspx.

[36] "ATI Industrial Automation," http://www.ati-ia.com/ http://www.ati-ia.com/products/ft/ft_models.aspx?id=Mini45 http://www.ati-ia.com/products/ft/ft_models.aspx?id=Omega85.

[37] "Point Grey Research," http://www.ptgrey.com/ http://ww2.ptgrey.com/firewire/dragonfly-2.

[38] "Scinamics," http://www.scinamics.com/.

[39] "Olympus," http://www.olympus.com/ http://www.olympus.de/site/de/a/audio_accessories/accessories_audio_recording/microphones_3/me_15/index.html.